Chemical Methodologies 8(2024) 72-84

Chemical Methodologies

Journal homepage: http://chemmethod.com

Original Article

Chloral Hydrate Adsorption on the Surface of Pristine and Al-doped Boron Nitride Nanoclusters: A Comprehensive and Comparative Theoretical Study

Pedram Niknam Rad[1], Saeid Abrahi Vahed[2], Mohammad Reza Jalali Sarvestani[3], Roya Ahmadi[4,*]

[1]*Department of Chemistry, Faculty of Science Hamedan Branch, Islamic Azad University, Hamedan, Iran*
[2]*Young Researchers and Elite Club, Tehran Medical Sciences, Islamic Azad University, Tehran, Iran*
[3]*Young Researchers and Elite Club, Yadegar-e-Imam Khomeini (RAH) Shahr-e-Rey Branch, Islamic Azad University, Tehran, Iran*
[4]*Department of Chemistry, Yadegar-e-Imam Khomeini (RAH) Shahre-Rey Branch, Islamic Azad University, Tehran, Iran*

ARTICLEINFO

Article history
Submitted: 2023-12-21
Revised: 2024-01-05
Accepted: 2024-01-13
Manuscript ID: CHEMM-2312-1751
Checked for Plagiarism: Yes
Language Checked: Yes

DOI:10.48309/CHEMM.2024.431534.1751

KEYWORDS
Chloral hydrate
Sensor
$B_{12}N_{12}$
DFT
B3LYP/6-31G (d)

ABSTRACT

This study investigated the potential of pristine and Al-doped BN nanoclusters ($B_{12}N_{12}$, $AlB_{11}N_{12}$) as adsorbents and sensing materials for the removal and detection of Chloral hydrate (CH) using density functional theory computations. The calculated values of adsorption energies, ΔG_{ad}, ΔH_{ad}, and K_{th} revealed that CH interaction with $B_{12}N_{12}$ is experimentally impossible, endothermic, and non-spontaneous. However, the CH adsorption on the $AlB_{11}N_{12}$ is exothermic, spontaneous, and experimentally feasible. The influence of solvent was also considered, and the results indicated that the presence of water does not significantly affect the interactions. Furthermore, the Natural Bond Orbital (NBO) computations showed that no chemical bond has formed between the adsorbate and adsorbent, indicating that the interactions between CH and both nanoclusters are due to physisorption. Moreover, frontier molecular orbital calculations indicated that while the bandgap of $B_{12}N_{12}$ remains largely unchanged during the CH adsorption process, the bandgap of $AlB_{11}N_{12}$ increases by 132.693% from 4.270 eV to 9.936 eV. In conclusion, the theoretical findings suggest that the Al-doped nanocluster, $AlB_{11}N_{12}$, has the potential to be an excellent adsorbent and sensor for the removal and detection of Chloral hydrate. This study provides valuable insights into the use of nanoclusters in environmental and analytical applications, highlighting the potential for developing efficient materials for CH removal and detection. Further experimental validation of these theoretical findings could pave the way for the practical application of Al-doped boron nitride nanoclusters in addressing environmental and analytical challenges associated with Chloral hydrate.

* Corresponding author: Roya Ahmadi
E-mail: roya_ahmadi_chem@yahoo.com

GRAPHICAL ABSTRACT

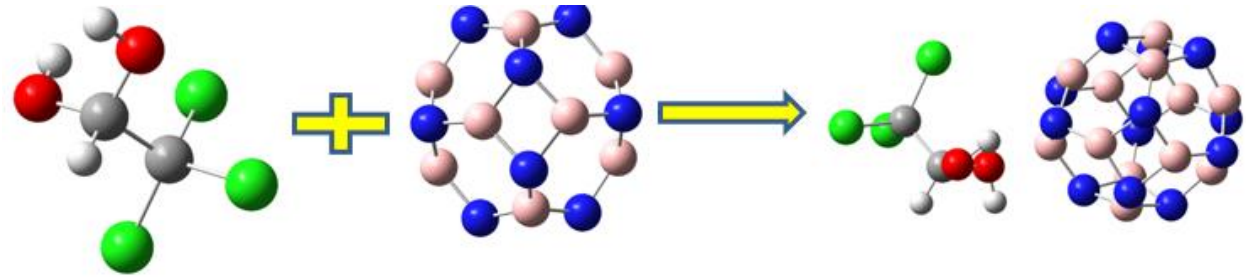

Introduction

Chloral hydrate (CH, Figure 1) is a hypnotic drug that was initially synthesized in 1832 by chemist Justus von Liebig. It is primarily used for the treatment of insomnia, anxiety, and as a sedative agent before certain medical procedures [1]. However, the use of CH is associated with several serious side effects, including nausea, allergic reactions, convulsions, kidney malfunction, liver failure, cardiac arrhythmia, and coma. Furthermore, patients often develop tolerance and addiction to CH [2]. In addition to its medical implications, CH can also be an undesired by-product in the chlorination step of drinking water treatment [3]. This is due to the presence of organic environmental contaminants in surface waters and their reaction with chlorine during the disinfection process [4]. The World Health Organization (WHO) has set a limit of 10 μg L^{-1} for CH in drinking water, as it has been found to have mutagenic and carcinogenic effects. Apart from its medical and environmental implications, CH is also used as a chemical reagent in the synthesis of various organic compounds [5,6]. Therefore, there is a need for a simple, selective, and cost-effective method for the determination and removal of CH. Several analytical techniques have been developed for the determination of CH, including UV-Visible spectrophotometry [7], gas-chromatography (GC) [8], anion-exchange liquid chromatography [9], and gas chromatography-mass spectrometry (GC-MS) [10]. However, these methods have their limitations, such as expensive instrumentation, time-consuming procedures, the requirement of experienced operators for sample pretreatment, and the use of toxic organic solvents. Electrochemical sensors are a promising alternative to traditional analytical techniques due to their small size, portability, and cost-effectiveness. They offer simple instrumentation, high selectivity and sensitivity, rapid analysis time, and a wide linear range for detecting various analyte concentrations. These sensors are valuable in environmental monitoring, healthcare diagnostics, and food safety testing. Their portability makes them suitable for on-site testing in remote areas. Ongoing technological developments are expected to enhance their capabilities further [11-13]. In addition to the CH determination, the removal of pharmaceutical contaminants from wastewater is also a significant concern. Various techniques have been employed for this purpose, including biological treatment [14], membrane filtration [15], electrochemical destruction [16], photocatalysis [17], advanced oxidation [18], reversed osmosis [19], ozonation [20], and disinfection [21]. However, these techniques have their drawbacks, such as high cost, limited removal capacity, harsh reaction conditions, time-consuming procedures, and the production of potential environmental contaminants as by-products [22]. Adsorption is an ideal alternative to these techniques due to its simplicity, low cost, versatility in adsorbent properties, high efficiency, and insensitivity towards hazardous materials, rapidness, flexibility, and ease of operation [23]. However, finding an adsorbent with high reusability, selectivity, and repeatability remains a challenge. In the development of new electrochemical sensors and

adsorbents for the detection and removal of CH or other analytes, it is crucial to find appropriate materials that have good and selective interactions with the desired compounds. This initial step is essential in ensuring the effectiveness and reliability of these methods. Overall, the determination and removal of CH are of great importance in both medical and environmental contexts. The development of simple and cost-effective analytical techniques, such as electrochemical sensors, along with efficient adsorbents for removal purposes, can contribute significantly to addressing these challenges [23]. Based on extensive research, boron nitride nanocage has been identified as possessing several highly desirable chemical and physical characteristics within the field of wide-gap semiconductors [24]. Numerous studies have evaluated the stability, geometry, and properties of boron nitride fullerenes, with $B_{12}N_{12}$ (Figure 1) emerging as the most stable cluster among various $(BN)_n$ nanoclusters [25]. $B_{12}N_{12}$, a compound with exceptional properties, has gained attention for its unique combination of characteristics. Its low dielectric constant makes it ideal for electronic applications by enabling efficient energy storage and transmission. In addition, its high thermal conductivity and good structural and thermal stability make it suitable for demanding environments. $B_{12}N_{12}$'s specific surface/area ratio is advantageous for catalytic applications, while its wide bandgap and excellent oxidation resistance further enhance its potential for use in optoelectronic devices and various technological applications. This material holds diverse possibilities in electronics, catalysis, and optoelectronics, showcasing potential innovation across multiple fields as research progresses [26].

These attributes position it as an ideal adsorbent for environmental contaminant removal and a promising candidate for detecting various analytes. Several investigations have explored the adsorption of different species on the surface of $B_{12}N_{12}$, including H_2S, nitroaromatic explosives, quetiapine, and Norfloxacin [27-30]. These findings underscore the potential of boron nitride nanocage in addressing environmental and analytical challenges.

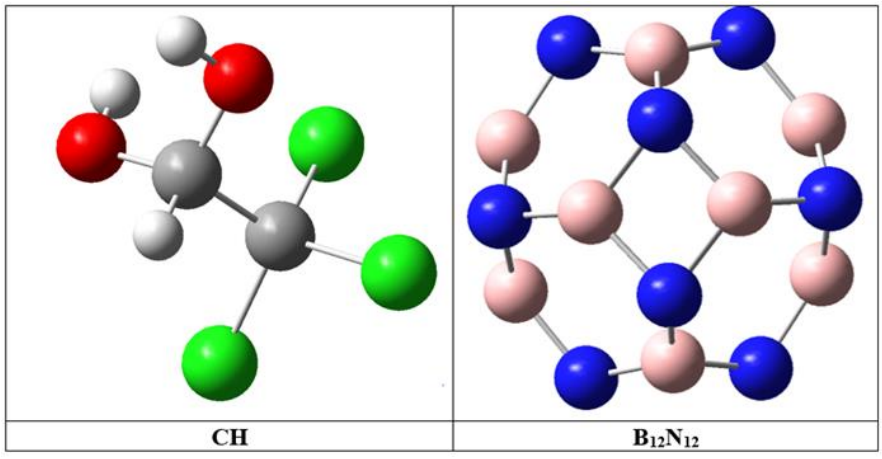

Figure 1: Optimized structures of CH and $B_{12}N_{12}$

Computational Methods

The structures of BN nanocage, CH, and their complexes were created using GuassView 6 [21] and Nanotube Modeler 1.3.0.3 [22]. The calculations were performed with the density functional theory (DFT) method in Gaussian 16 [23] software at the B3LYP/6-31G (d) level of theory [24]. The parameters were determined following a method outlined in [25-30].

Software versions GuassView 6 [31] and Nanotube Modeler 1.3.0.3 [32] were utilized to design the structures of $B_{12}N_{12}$, $AlB_{11}N_{12}$, CH, and their complexes. Prior to any further analysis, each of the designed structures underwent geometric optimization. Subsequently,

computations for infra-red (IR), frontier molecular orbital (FMO), and natural bond orbital (NBO) were performed on the optimized structures. The density functional theory (DFT) method was consistently employed throughout the computations using Gaussian 16 [33] software, employing the B3LYP/6-31G (d) Basis set [34]. To obtain the density of states (DOS) spectra, GuassSum 3.0 software was utilized [35]. This level of theory was selected based on its previous acceptance and alignment with experimental results [36-40]. All computations were conducted in both vacuum and aqueous phases, with the CPCM solvation method chosen for modeling the aqueous phase. The temperature range investigated spanned from 298 to 398 K, with intervals of 10˚. The main focus of this investigation was the process of drug adsorption onto an adsorbent material, which can be represented by the following equation [30]:

$$\text{Drug} + \text{Adsorbent} \rightarrow \text{Drug-Adsorbent} \quad (1)$$

To evaluate the strength of the drug-adsorbent interaction, adsorption energy values (E_{ad}) and various thermodynamic parameters were calculated. These thermodynamic parameters include the thermodynamic equilibrium constant (K_{th}), Gibbs free energy changes (ΔG_{ad}), and adsorption enthalpy changes (ΔH_{ad}). The calculations of these parameters were carried out using equations 2–6 [41].

$$E_{ad} = \left(E_{(Complex)} - \left(E_{(Drug)} + E_{(Adsorbent)+}E_{(BSSE)}\right)\right) \quad (2)$$

$$\Delta H_{ad} = \left(H_{(Complex)} - \left(H_{(Drug)} + H_{(Adsorbent)}\right)\right) \quad (3)$$

$$\Delta G_{ad} = \left(G_{(Complex)} - \left(G_{(Drug)} + G_{(Adsorebnt)}\right)\right) \quad (4)$$

$$\Delta S_{ad} = \left(S_{(Complex)} - \left(H_{(Drug)} + H_{(Adsorbent)}\right)\right) \quad (5)$$

$$K_{th} = \left(exp - \left(\Delta G_{ad}/RT\right)\right) \quad (6)$$

Overall, the software tools and computational methods employed in this study allowed for the design and analysis of various structures and their complexes. The investigation focused on understanding the drug-adsorbent interaction through the calculation of adsorption energy values and thermodynamic parameters. The results obtained from these calculations will contribute to a better understanding of the adsorption process and provide valuable insights for future drug design and development efforts. In the aforementioned equations, the variable E represents the total electronic energy for each structure being studied. EBSSE, on the other hand, denotes the basis set superposition correction. The variable H encompasses the total energy of the evaluated materials along with the thermal correction of enthalpy. Similarly, G symbolizes the total energy plus the thermal correction of the Gibbs free energy, as described in reference. R refers to the constant of the ideal gas, while S represents the thermal correction entropy for the structures under investigation. Lastly, T corresponds to the temperature, as outlined in reference [42]. These equations, specifically equations 7–12, are utilized for the computation of several crucial properties. The bandgap (Eg), chemical hardness (η), chemical potential (μ), the maximum charge capacity (ΔN_{max}), and electrophilicity (ω) of frontier molecular orbitals are all calculated using these equations [42].

$$E_g = E_{LUMO} - E_{HOMO} \quad (7)$$

$$\%\Delta E_g = \frac{E_{g2}-E_{g1}}{Eg1} \times 100 \quad (8)$$

$$\eta = {(E_{LUMO} - E_{HOMO})}/{2} \quad (9)$$

$$\mu = {(E_{LUMO} + E_{HOMO})}/{2} \quad (10)$$

$$\omega = {\mu^2}/{2\eta} \quad (11)$$

$$\Delta N_{max} = -{\mu}/{\eta} \quad (12)$$

In the given equations, E_{LUMO} represents the energy of the lowest unoccupied molecular orbital, while E_{HOMO} represents the energy of the highest occupied molecular orbital. The bandgaps of the Nano-adsorbent and CH-Adsorbent complexes are denoted as Eg_1 and Eg_2, respectively [42].

Results and Discussion

Structural and NBO Analysis

The provided initial and optimized structures in Figures 2 and 3 clearly demonstrate that there were no significant structural deformations in the complexes of CH with pristine and Al-doped nanocages after geometrical optimizations. This indicates that no chemical bond has formed between the adsorbate and the adsorbent during the adsorption process of CH [27]. To determine the most stable configuration, the interactions were studied at three different geometries. In the A and Al-A conformers, CH was inserted near the $B_{12}N_{12}$ and $AlB_{11}N_{12}$ cages, respectively, towards its chlorine atoms. In the B and Al-B conformers, the adsorbate was located near the pristine and Al-doped adsorbents, respectively, towards its side view (from one of the chlorines and one of the hydroxyl groups). In the C and Al-C conformers, CH was placed near the $B_{12}N_{12}$ and $AlB_{11}N_{12}$ cages towards its hydroxyl groups. The calculated values of total electronic energies and adsorption energies are presented in Table 1.

As demosnrtated, the adsorption energies are positive in the case of the pristine nanocage, indicating that the interaction between CH and the pristine BN nanocage is experimentally impossible. However, for $AlB_{11}N_{12}$, the adsorption energies are highly negative; indicating that CH interaction with Al-doped nanocluster is experimentally feasible [28]. Amongst the studied configurations, the Al-B conformer has the most negative total electronic energy, suggesting that the formation of this configuration is more energetically favourable than the others. All of the investigated structures underwent IR calculations, and the obtained the minimum and the maximum frequencies are listed in Table 1. It is worth noting that no negative frequencies were observed, indicating that all of the scrutinized structures are true local minimums [29]. The dipole moments of the CH molecule before and after adsorption on the surfaces of $B_{12}N_{12}$ and $AlB_{11}N_{12}$ cages are shown in Table 1. It is observed that the dipole moment of CH increases after adsorption on both nanocages, indicating that the CH complexes with these nanocages are expected to be more soluble in polar solvents compared to the pure drug without nanostructure [30]. To further understand the adsorption mechanism, NBO computations were performed on the structures. The results indicate that no chemical bond has been formed between the drug and the nanostructures, and the nature of interactions is physisorption in both cases [40].

Table 1: The calculated values structural parameters

	Total electronic energy (a.u)	Adsorption energy (kcal/mol)	Zero-point energy (kcal/mol)	Maximum IR frequency (cm^{-1})	Minimum IR frequency (cm^{-1})	Dipole Moment (Debye)
CH	-1609.019	---	35.594	100.470	3744.456	2.210
$B_{12}N_{12}$	-956.146	---	81.134	322.349	1446.729	0.000
A-Conformer	-2565.202	107.335	116.777	110.980	2075.230	2.230
B-Conformer	-2565.215	100.523	117.548	201.600	2066.260	3.350
C-Conformer	-2565.223	96.101	117.910	213.050	2062.670	2.850
$AlB_{11}N_{12}$	-1173.727	---	78.370	240.100	1446.712	3.240
Al-A-Conformer	-2782.806	-36.085	113.907	130.790	2059.340	11.557
Al-B-Conformer	-2782.839	-43.098	114.568	202.810	2057.280	7.142
Al-C-Conformer	-2782.797	-30.166	114.566	197.830	2049.360	2.960

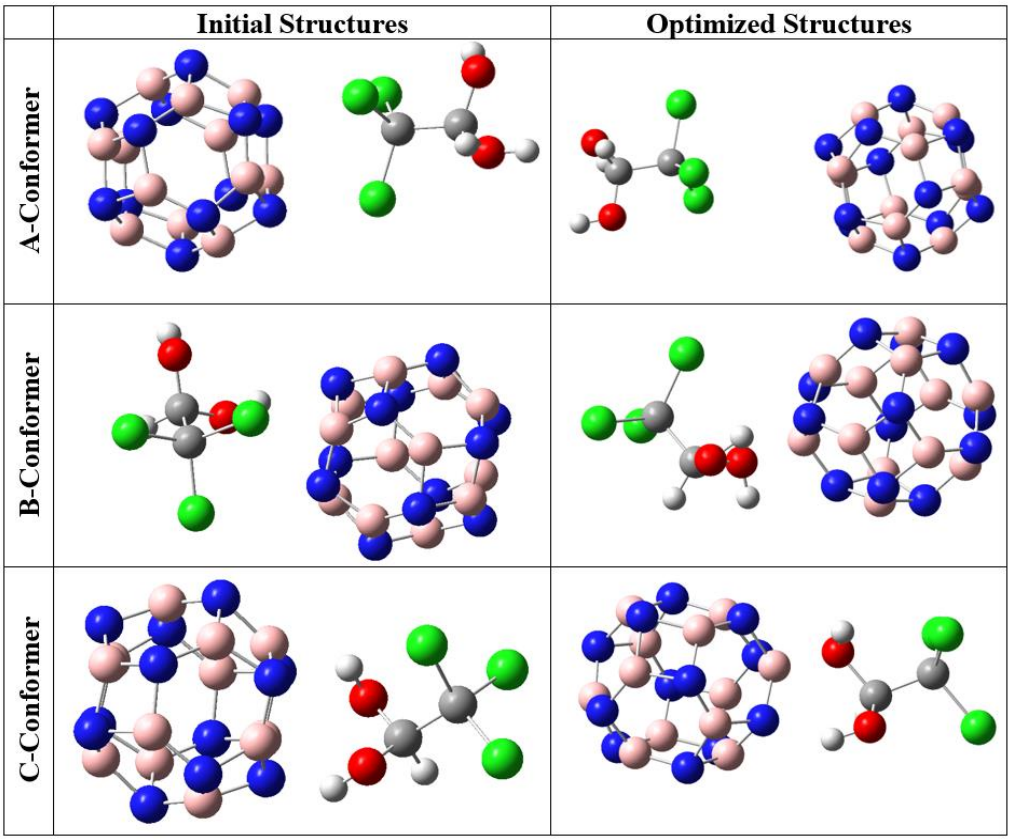

Figure 2: The initial and optimized structures of CH-$B_{12}N_{12}$ complexes

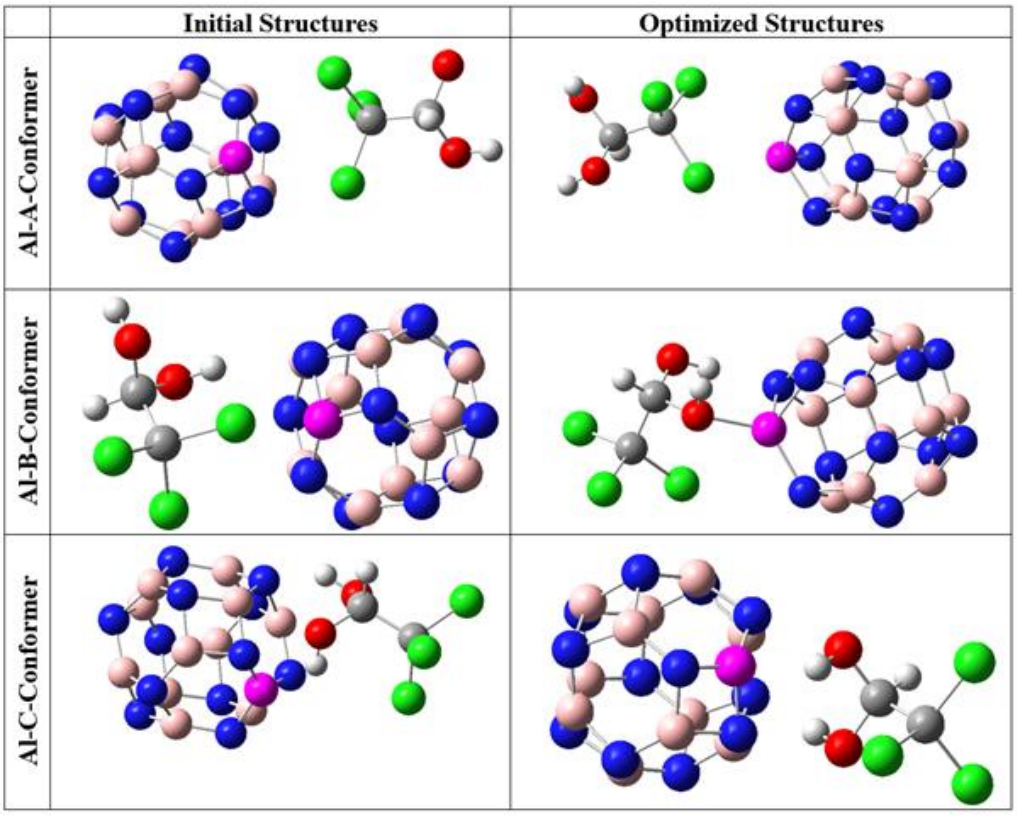

Figure 3: The initial and optimized structures of CH-$AlB_{11}N_{12}$ complexes

These findings suggest that the interaction between CH and the $B_{12}N_{12}$ and $AlB_{11}N_{12}$ cages is primarily physical in nature, rather than forming chemical bonds. This information is valuable for understanding the behaviour of CH when interacting with these nanocages, particularly in terms of solubility in different solvents. Overall, the increase in dipole moment and the nature of interactions between CH and the nanocages provide important insights into the potential applications of these complexes, particularly in drug delivery and solubility enhancement.

Thermodynamic Parameters

Thermochemical parameters for the CH adsorption of on the surfaces of $B_{12}N_{12}$ and $AlB_{11}N_{12}$ have been calculated and presented in Table 2. The aim of this study was to gain a deeper understanding of the thermodynamics of the adsorption process on these nanoclusters. The results indicate that the interaction of CH with $B_{12}N_{12}$ is non-spontaneous, endothermic, and thermodynamically inappropriate. This is evidenced by the positive values of ΔH_{ad}, ΔG_{ad} and the negligible values of Kth observed in the cases of A, B, and C conformers. In contrast, the interaction of CH with Al-doped nanocluster is exothermic, spontaneous, and reversible [40]. This is indicated by the achieved negative values of ΔH_{ad}, ΔG_{ad} and the substantial values of Kth observed in the cases of Al-A, Al-B, and Al-C conformers. It should be noted that the negative values of ΔS_{ad} observed in both cases show that the adsorption process on both nanoclusters is inappropriate in terms of entropy [40]. This may be attributed to the aggregation of complexes after interaction with both adsorbents. Overall, these findings provide valuable insights into the thermodynamics of CH adsorption on $B_{12}N_{12}$ and $AlB_{11}N_{12}$ nanoclusters, which may have important implications for future research in this area.

Table 2: Thermodynamic parameters of the adsorption process

NO	ΔH_{ad} (kcal/mol)	ΔG_{ad} (kcal/mol)	ΔS_{ad} (cal/mol.K)	K_{th}
A-Conformer	108.164	116.385	-28.285	2.282×10^{-86}
B-Conformer	100.671	114.258	-42.510	8.381×10^{-85}
C-Conformer	96.499	110.030	-42.323	1.083×10^{-81}
Al-A-Conformer	-36.036	-25.725	-31.616	$8.505\times10^{+18}$
Al-B-Conformer	-43.084	-29.822	-41.472	$8.807\times10^{+21}$
Al-C-Conformer	-30.118	-19.807	-31.616	$3.756\times10^{+14}$

FMO Analysis

The DOS spectra of $B_{12}N_{12}$ and its complexes with CH are given in Figure 4. It can be observed that the bandgap of the BN nanocage is 6.830 eV. However, when CH is adsorbed on its surface, the bandgap decreases to 6.305 eV, 5.670 eV, and 5.442 eV in A, B, and C conformers respectively, representing a decline of approximately 7.687%, 16.988%, and 20.328%. Similarly, the DOS spectra of $AlB_{11}N_{12}$ and its complexes with CH are shown in Figure 5. The bandgap of $AlB_{11}N_{12}$ is initially 4.270 eV. Upon interaction with CH, this parameter increases to 4.922 eV, 5.829 eV, and 9.936 eV, corresponding to an increase of approximately 15.278%, 36.518%, and 132.693%, respectively. The bandgap of a compound is inversely related to its electrochemical conductivity. A molecule with a narrow bandgap exhibits higher conductivity compared to a compound with a wider bandgap [40]. Therefore, significant changes in the bandgap can serve as an analytical signal for the detection of the desired analyte, in this case, CH. In this regard, $AlB_{11}N_{12}$ appears to be a more suitable sensing material for the detection of CH as its bandgap is lower than that of $B_{12}N_{12}$, indicating higher conductivity in the Al-doped nanocage. Furthermore, the variations in bandgap after CH adsorption are more pronounced in the case of $AlB_{11}N_{12}$ compared to

$B_{12}N_{12}$ [40]. Additional quantum chemistry parameters such as chemical potential, chemical hardness, electrophilicity, and the maximum transferred charge were also calculated and are reported in Table 3. The negative values for the chemical potential indicate that all of the studied structures are thermodynamically stable [40]. The chemical hardness of CH is 3.495 eV, and when it interacts with $B_{12}N_{12}$ and $AlB_{11}N_{12}$, this parameter experiences a slight decrease in all of the complexes.

Chemical hardness is inversely proportional to chemical reactivity, meaning that a compound with lower chemical hardness is more reactive than one with a higher value [40]. Therefore, it can be inferred that CH complexes with both nanoclusters exhibit higher chemical reactivity compared to pure CH without any nanocage. The calculated values of electrophilicity and the maximum transferred charge are also provided in Table 3. Both indices indicate the tendency of a molecule to absorb electrons. It is evident from the table that both indices for CH show a significant increase after interaction with both nanoclusters. Thus, it can be concluded that CH complexes with $B_{12}N_{12}$ and $AlB_{11}N_{12}$ are more electrophilic than pure CH without any nanostructures [41, 42].

Overall, the analysis of the DOS spectra and quantum chemistry parameters suggests that both $B_{12}N_{12}$ and $AlB_{11}N_{12}$ nanoclusters have unique properties when interacting with CH, making them potential candidates for sensing applications or other relevant fields.

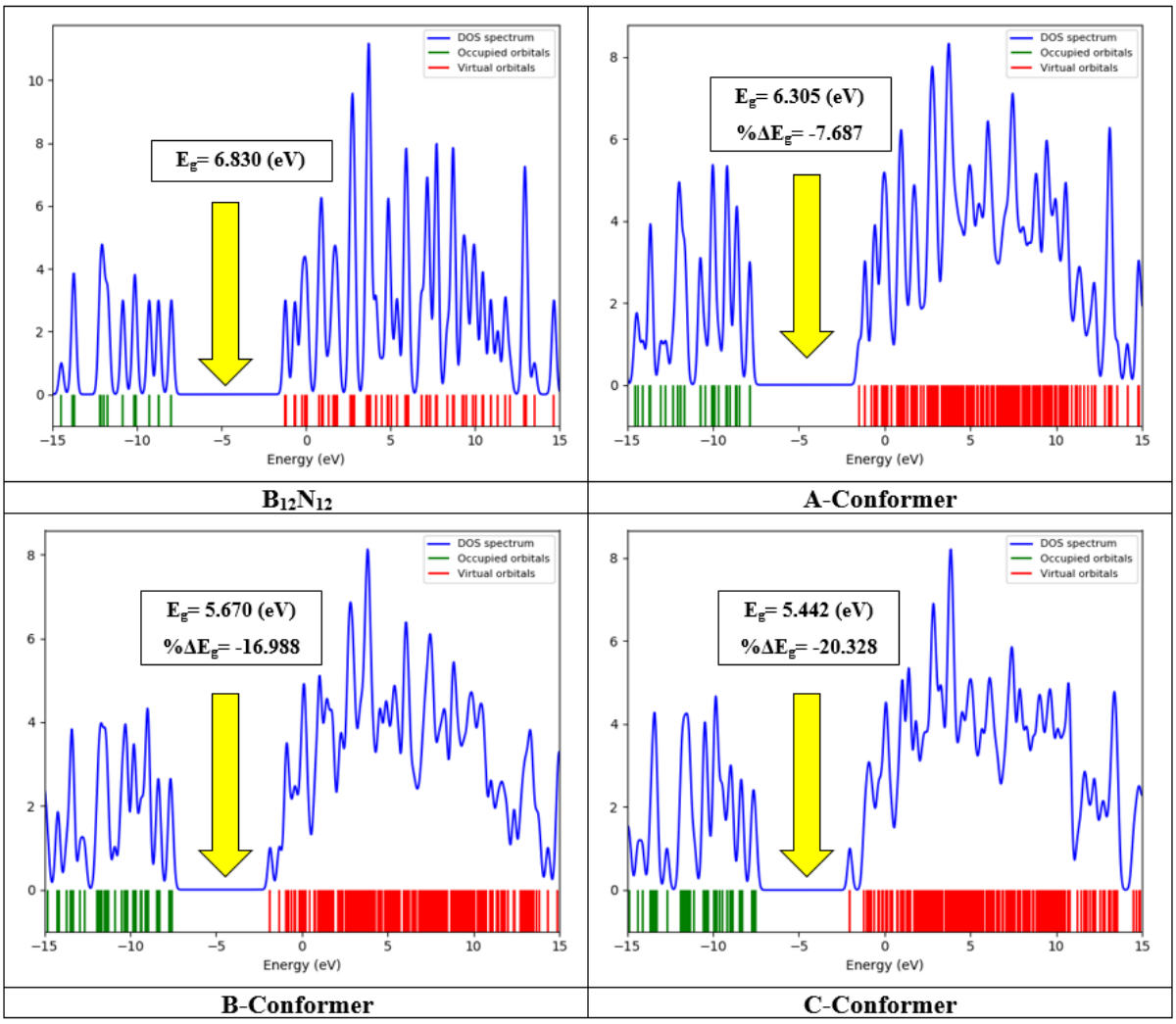

Figure 4: DOS spectrums of $B_{12}N_{12}$ and its complexes with CH

Table 3: The calculated FMO parameters for CH, $B_{12}N_{12}$, $AlB_{11}N_{12}$, and their complexes

No.	EHOMO (eV)	ELUMO (eV)	Eg (eV)	%Δeg	η (eV)	μ (eV)	ω (eV)	ΔNmax (eV)
CH	-8.150	2.160	10.310	---	5.155	-2.995	0.870	0.581
$B_{12}N_{12}$	-7.700	-0.870	6.830	---	3.415	-4.285	2.688	1.255
A-Conformer	-7.787	-1.482	6.305	-7.687	3.153	-4.635	3.407	1.470
B-Conformer	-7.506	-1.836	5.670	-16.988	2.835	-4.671	3.848	1.648
C-Conformer	-7.450	-2.008	5.442	-20.328	2.721	-4.729	4.110	1.738
$AlB_{11}N_{12}$	-7.310	-3.040	4.270	---	2.135	-5.175	6.272	2.424
Al-A-Conformer	-7.158	-2.235	4.922	15.278	2.461	-4.697	4.481	1.908
Al-B-Conformer	-7.380	-1.551	5.829	36.518	2.915	-4.466	3.421	1.532
Al-C-Conformer	-10.038	-0.102	9.936	132.693	4.968	-5.070	2.587	1.021

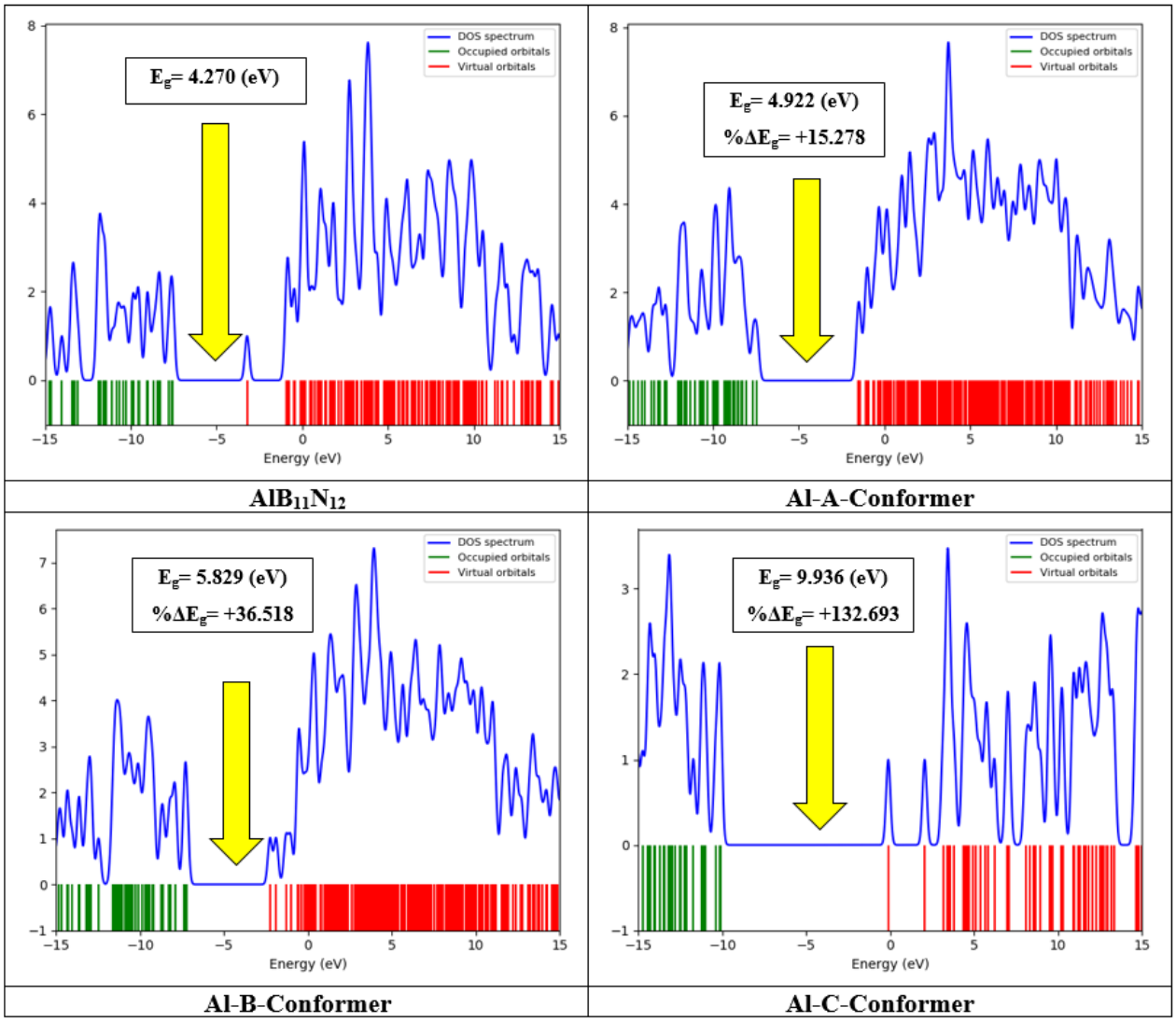

Figure 5: DOS spectrums of $AlB_{11}N_{12}$ and its complexes with CH

Conclusion

The study investigated the potential of pristine and Al-doped boron nitride nanoclusters ($B_{12}N_{12}$ and $AlB_{11}N_{12}$) as adsorbents and sensing materials for the removal and detection of CH using density functional theory computations. The findings indicate that the interaction of CH with $B_{12}N_{12}$ is experimentally impossible, as it is characterized by endothermic and non-spontaneous behaviour. Conversely, the adsorption of CH on $AlB_{11}N_{12}$ is experimentally feasible and exhibits exothermic and spontaneous characteristics. This suggests that Al-doped nanoclusters, especially $AlB_{11}N_{12}$, hold promise as effective adsorbents and sensors for CH removal and detection. Our results revealed that the presence of water does not significantly impact the CH interactions with the nanoclusters. This implies that the proposed materials can maintain stability and effectiveness even in the presence of water, enhancing their practical applicability. The NBO computations demonstrated that no chemical bond has formed between adsorbate and adsorbent, and CH interactions with both nanoclusters are physisorption. Moreover, the frontier molecular orbital calculations exhibited that while the bandgap of $B_{12}N_{12}$ does not undergo substantial changes during the adsorption process of CH, the bandgap of $AlB_{11}N_{12}$ does experience a significant increase of 132.693% from 4.270 eV to 9.936 eV. This noteworthy increase in bandgap strengthens the $AlB_{11}N_{12}$potential as a sensing material for the CHdetection.

Overall, the theoretical findings of this study suggest that Al-doped boron nitride nanoclusters, particularly $AlB_{11}N_{12}$, hold great promise as excellent adsorbents and sensors for the removal and detection of CH. Further experimental investigations should be conducted to validate these theoretical predictions and explore the practical applications of these materials in environmental and analytical chemistry.

ORCID

Roya Ahmadi
https://orcid.org/0000-0002-0002-7858

References

[1]. Fairbrother J.E., Chloral Hydrate, *Analytical Profiles of Drug Substances and Excipients,* 1973, **2**:85 [Crossref], [Google Scholar], [Publisher]
[2]. Luknitskii F.I., The Chemistry of Chloral, *Chemical Reviews*, 1975, **75**:259 [Crossref], [Google Scholar], [Publisher]
[3]. Paparella S.F., Chloral hydrate: safety risks still worth mentioning, *Journal of Emergency Nursing*, 2018, **44**:81 [Crossref], [Google Scholar], [Publisher]
[4]. Dąbrowska A., Nawrocki J., Controversies about the occurrence of chloral hydrate in drinking water, *Water research*, 2009, **43**:2201 [Crossref], [Google Scholar], [Publisher]
[5]. Friedman P., Cooper J., Determination of ChloralHydrate, Trichloroacetic Acid, and Trichloroethanol, *Analytical Chemistry*, 1958, **30**:1674 [Crossref], [Google Scholar], [Publisher]
[6]. Schmitt T.C., Determination of chloral hydrate and its metabolites in blood plasma by capillary gas chromatography with electron capture detection, *Journal of Chromatography B*, 2002, **780**:217 [Crossref], [Google Scholar], [Publisher]
[7]. Bruzzoniti M.C., Mentasti E., Sarzanini C., Tarasco E., Liquid chromatographic methods for chloral hydrate determination, *Journal of Chromatography a*, 2001, **920**:283 [Crossref], [Google Scholar], [Publisher]
[8]. Yan Z., Henderson G.N., James M.O., Stacpoole P.W., Determination of chloral hydrate metabolites in human plasma by gas chromatography-mass spectrometry, *Journal of pharmaceutical and biomedical analysis*, 1999, **19**:309 [Crossref], [Google Scholar], [Publisher]
[9]. Iorhuna F., Ayuba A.M., Muhammad A.S., Computational Studies on the Corrosion Inhibition of Mild Steel Using Pyrimidine Derivatives, 2023, [Crossref], [Google Scholar]
[10]. Ozkendir O.M., Mirzaei M., Alkali Metal Chelation by 3–Hydroxy–4–Pyridinone. *Advanced Journal of Chemistry-Section B: Natural Products*

and Medical Chemistry, 2019, **1:** 10 [Crossref], [Google Scholar]
[11]. Bakker E., Telting-Diaz M., Electrochemical sensors, *Analytical Chemistry*, 2002, **74**:2781 [Crossref], [Google Scholar], [Publisher]
[12]. Baghapour M.A., Shirdarreh M.R., Faramarzian M., Amoxicillin removal from aqueous solutions using submerged biological aerated filter, *Desalination and Water Treatment*, 2015, **54**:790 [Crossref], [Google Scholar], [Publisher]
[13]. Moarefian A., Golestani H.A., Bahmanpour H., Removal of amoxicillin from wastewater by self-made Polyethersulfone membrane using nanofiltration, *Journal of Environmental Health Science and Engineering*, 2014, **12**:1 [Crossref], [Google Scholar], [Publisher]
[14] Tan T.Y., Zeng Z.T., Zeng G.M., Gong J.L., Xiao R., Zhang P., Song B., Tang W.W., Ren X.Y., Electrochemically enhanced simultaneous degradation of sulfamethoxazole, ciprofloxacin and amoxicillin from aqueous solution by multi-walled carbon nanotube filter, *Separation and Purification Technology*, 2020, **235**:116167 [Crossref], [Google Scholar], [Publisher]
[15]. Tran M.L., Fu C.C., Juang R.S., Removal of metronidazole and amoxicillin mixtures by UV/TiO2 photocatalysis: an insight into degradation pathways and performance improvement, *Environmental Science and Pollution Research*, 2019, **26**:11846 [Crossref], [Google Scholar], [Publisher]
[16]. Ay F., Kargi F., Advanced oxidation of amoxicillin by Fenton's reagent treatment, *Journal of Hazardous Materials*, 2010, **179**:622 [Crossref], [Google Scholar], [Publisher]
[17]. Gholami M., Mirzaei R., Kalantary R.R., Sabzali A., Gatei F., Performance evaluation of reverse osmosis technology for selected antibiotics removal from synthetic pharmaceutical wastewater, *Iranian Journal of Environmental Health Science & Engineering*, 2012, **9**:1 [Crossref], [Google Scholar], [Publisher]
[18]. Andreozzi R., Canterino M., Marotta R., Paxeus N., Antibiotic removal from wastewaters: the ozonation of amoxicillin, *Journal of Hazardous Materials*, 2005, **122**:243 [Crossref], [Google Scholar], [Publisher]
[19]. Saravanamoorthy S., Banu M., Rachel Joy R., Computational analysis and molecular docking study of 4-(carboxyamino)-3-guanidino-benzoic acid. *Advanced Journal of Chemistry-Section B: Natural Products and Medical Chemistry*, 2021, **3**:120 [Crossref], [Google Scholar]
[20]. Merajoddina M., Pirib S., Mokarianc Z., Piria F., Density functional theory study of benzoic acid decarboxylation, *Asian Journal of Green Chemistry*, 2021, **5**:335 [Crossref], [Google Scholar]
[21]. Sarvestani M.R.J., Vahed S.A., Ahmadi R., Cefalexin adsorption on the surface of pristine and Al-doped boron nitride nanocages ($B_{12}N_{12}$ and $AlB_{11}N_{12}$): A theoretical study, *South African Journal of Chemical Engineering*, 2024, **47**:60 [Crossref], [Google Scholar], [Publisher]
[22]. Wu X., Yang J., Zeng X.C., Adsorption of hydrogen molecules on the platinum-doped boron nitride nanotubes, *The Journal of Chemical Physics*, 2006, **125**:1 [Crossref], [Google Scholar], [Publisher]
[23]. Arenal R., Lopez-Bezanilla A., Boron nitride materials: an overview from 0D to 3D (nano) structures, *Wiley Interdisciplinary Reviews: Computational Molecular Science*, 2015, **5**:299 [Crossref], [Google Scholar], [Publisher]
[24]. Saboor F.H., Ataei A., Decoration of Metal Nanoparticles and Metal Oxide Nanoparticles on Carbon Nanotubes. *Advanced Journal of Chemistry, Section A*, 2024, **7**:122 [Crossref], [Publisher]
[25]. Semire B., Obiyenwa K., Anthony W., Muhammed A., Godwin M., Fagbenro S., Afolabi S., Salawu O. Manipulation of 2-[2-(10H-phenothiazin-3-yl)thiophen-3-yl]-10H-phenothiazine Based D-A-π -A Dyes for Effective Tuning of Optoelectronic Properties and Intramolecular Charge Transfer in Dye Sensitized Solar Cells: A DFT/TD-DFT Approach. *Advanced Journal of Chemistry, Section A*, 2024, **7:**41 [Crossref], [Publisher]
[26]. Shehu U., Usman B., Corrosion Inhibition of Iron Using Silicate Base Molecules: A Computational Study, *Advanced Journal of*

Chemistry, Section A, 2023, **6**:334 [Crossref], [Google Scholar], [Publisher]
[27]. Jalali Sarvestani M.R., Qomi M., Arabi S., Norfloxacin Adsorption on the Surface of $B_{12}N_{12}$ and Al12N12 Nanoclusters: A Comparative DFT Study, *Nanomedicine Research Journal*, 2023, **8**:393 [Crossref], [Google Scholar], [Publisher]
[28]. Frisch Æ., Gaussian 09W Reference. *Journal of the American Chemical Society,* 2009 [Google Scholar]
[29]. Melchor S., Dobado J.A., CoNTub: An algorithm for connecting two arbitrary carbon nanotubes, *Journal of chemical information and computer sciences*, 2004, **44**:1639 [Crossref], [Google Scholar], [Publisher]
[30]. O'boyle N.M., Tenderholt A.L., Langner K.M., Cclib: a library for package-independent computational chemistry algorithms, *Journal of computational chemistry*, 2008, **29**:839 [Crossref], [Google Scholar], [Publisher]
[31]. Frisch M.J., Trucks G.W., Schlegel H.B., Scuseria G.E., Robb M. a., Cheeseman J.R., Scalmani G., Barone V., Petersson G. a., Nakatsuji H., Li, X., Caricato M., Marenich A. V., Bloino J., Janesko B.G., Gomperts R., Mennucci B., Hratchian H.P., Ortiz J. V., Izmaylov a. F., Sonnenberg J.L., Williams Ding F., Lipparini F., Egidi F., Goings J., Peng B., Petrone A., Henderson T., Ranasinghe D., Zakrzewski V.G., Gao J., Rega N., Zheng G., Liang W., Hada M., Ehara M., Toyota K., Fukuda R., Hasegawa J., Ishida M., Nakajima T., Honda Y., Kitao O., Nakai H., Vreven T., Throssell K., Montgomery J.r., Peralta J.E., Ogliaro F., Bearpark M.J., Heyd J.J., Brothers E.N., Kudin K.N., Staroverov V.N., Keith T. a., Kobayashi R., Normand J., Raghavachari K., Rendell a. P., Burant J.C., Iyengar S.S., Tomasi J., Cossi M., Millam J.M., Klene M., Adamo C., Cammi R., Ochterski J.W., Martin R.L., Morokuma K., Farkas O., Foresman J.B., Fox D.J. G16_C01. Gaussian 16, Revision C.01, Gaussian, Inc., Wallin. (2016).
[32]. Ghiasi R., Aghazadeh Kozeh Kanani F., Theoretical insights of the electronic structures, conductivity, and aromaticiy of Graphyne and Si-doped Graphynes, *Journal of Medicinal and Nanomaterials Chemistry*, 2022, **4**:303 [Crossref], [Google Scholar], [Publisher]
[33]. Sarvestani M.J.,Ahmadi, R., Adsorption of TNT on the surface of pristine and N-doped carbon nanocone: A theoretical study, *Asian Joirnal of Nanoscience and Materials*, 2020, **3**:103 [Crossref], [Google Scholar]
[34]. Silva A.L.P., Sousa N. de, Jesus Gomes Varela Júnior J. de, Theoretical studies with $B_{12}N_{12}$ as a toxic gas sensor: a review, *Journal of Nanoparticle Research*, 2023, **25**:1 [Crossref], [Google Scholar], [Publisher]
[35]. Rezaei-Sameti M., Amirian B., A Quantum, NBO, RDG study of interaction cadmium ion with the pristine, C, P and C&P doped (4, 4) armchair boron nitride nanotube (BNNTs), *Asian Joirnal of Nanoscience and Materials*, 2018, **1**:262 [Crossref], [Google Scholar]
[36]. Afshar M., Khojasteh R.R., Ahmadi R., Adsorption of lomustin anticancer drug on the surface of carbon nanotube: A theoretical study, *Eurasian Chemical Communications*, 2020, **2**:595 [Crossref], [Google Scholar]
[37]. Shahzad H., Ahmadi R., Adhami F., Najafpour J., Adsorption of Cytarabine on the Surface of Fullerene C20: A Comprehensive DFT Study, *Eurasian Chemical Communications,* 2020, **2**:162 [Crossref], [Google Scholar]
[38]. Bedassa T.,Desalegne, M., Assessment of selected physico-chemical properties and metals in Qeera stream water, Bakkee-Jamaa, Nekemte, Ethiopia, *International Journal of New Chemistry*, 2020, **7**:47 [Crossref], [Google Scholar], [Publisher]
[39]. Abrahi Vahed S., Hemmati Tirabadi F., A DFT Investigation on Fullerene (C_{20}) Interaction with Nalidixic Acid, *International Journal of New Chemistry*, 2022, **9**:393 [Crossref], [Google Scholar], [Publisher]
[40]. Rezaei Sameti M.,Barandisheh Naghibi, M., A quantum assessment of the interaction between $Si_{12}C_{12}$, $BSi_{11}C_{12}$, $BSi_{12}C_{11}$, $NSi_{11}C_{12}$ and NSi12C11 nanocages with Glycine amino acid: A DFT, TD-DFT and AIM study, *International Journal of New Chemistry*, 2023, **11**:15 [Crossref], [Google Scholar], [Publisher]
[41]. Sharma G., Sharma S.B., Synthetic Impatienol analogues as potential cyclooxygenase-2 inhibitors: a preliminary study,

Journal of Applied Organometallic Chemistry, 2021, **1**:66 [Crossref], [Publisher]
[42]. Farhami N., A computational study of thiophene adsorption on boron nitride nanotube, *Journal of Applied Organometallic Chemistry*, 2020, **8**:249 [Crossref], [Publisher]

HOW TO CITE THIS ARTICLE
Pedram Niknam Rad, Saeid Abrahi Vahed, Mohammad Reza Jalali Sarvestani, Roya Ahmadi. Chloral Hydrate Adsorption on the Surface of Pristine and Al-doped Boron Nitride Nanoclusters: A Comprehensive and Comparative Theoretical Study. *Chem. Methodol.*, 2024, 8(2) 72-84
DOI: https://doi.org/10.48309/CHEMM.2024.431534.1751
URL: https://www.chemmethod.com/article_187402.html